Supplement of

The fate of fixed nitrogen in Santa Barbara Basin sediments during seasonal anoxia

Xuefeng Peng[1,2,3], David J. Yousavich[4], Annie Bourbonnais[1], Frank Wenzhoefer[5,6,7], Felix Janβen[5,6], Tina Treude[4,8] and David L. Valentine[2,3]

[1]School of Earth, Ocean and Environment, University of South Carolina, 701 Sumter Street, Columbia, SC, USA

[2]Marine Science Institute, University of California, Santa Barbara, CA, USA

[3]Department of Earth Science, 1006 Webb Hall, University of California, Santa Barbara, CA, USA

[4]Department of Earth, Planetary, and Space Sciences, University of California Los Angeles, 595 Charles E. Young Drive East, Los Angeles, CA, USA

[5]HGF-MPG Group for Deep-Sea Ecology and Technology, Alfred-Wegener-Institute, Helmholtz-Center for Polar and Marine Research, Am Handelshafen 12, Bremerhaven, Germany

[6]Max Planck Institute for Marine Microbiology, Celsiusstrasse 1, Bremen, Germany

[7]Department of Biology, DIAS, Nordcee and HADAL Centres, University of Southern Denmark, Odense M, Denmark

[8]Department of Atmospheric and Oceanic Sciences, University of California Los Angeles, Math Science Building, 520 Portola Plaza, Los Angeles, CA, USA.

Contents of this file
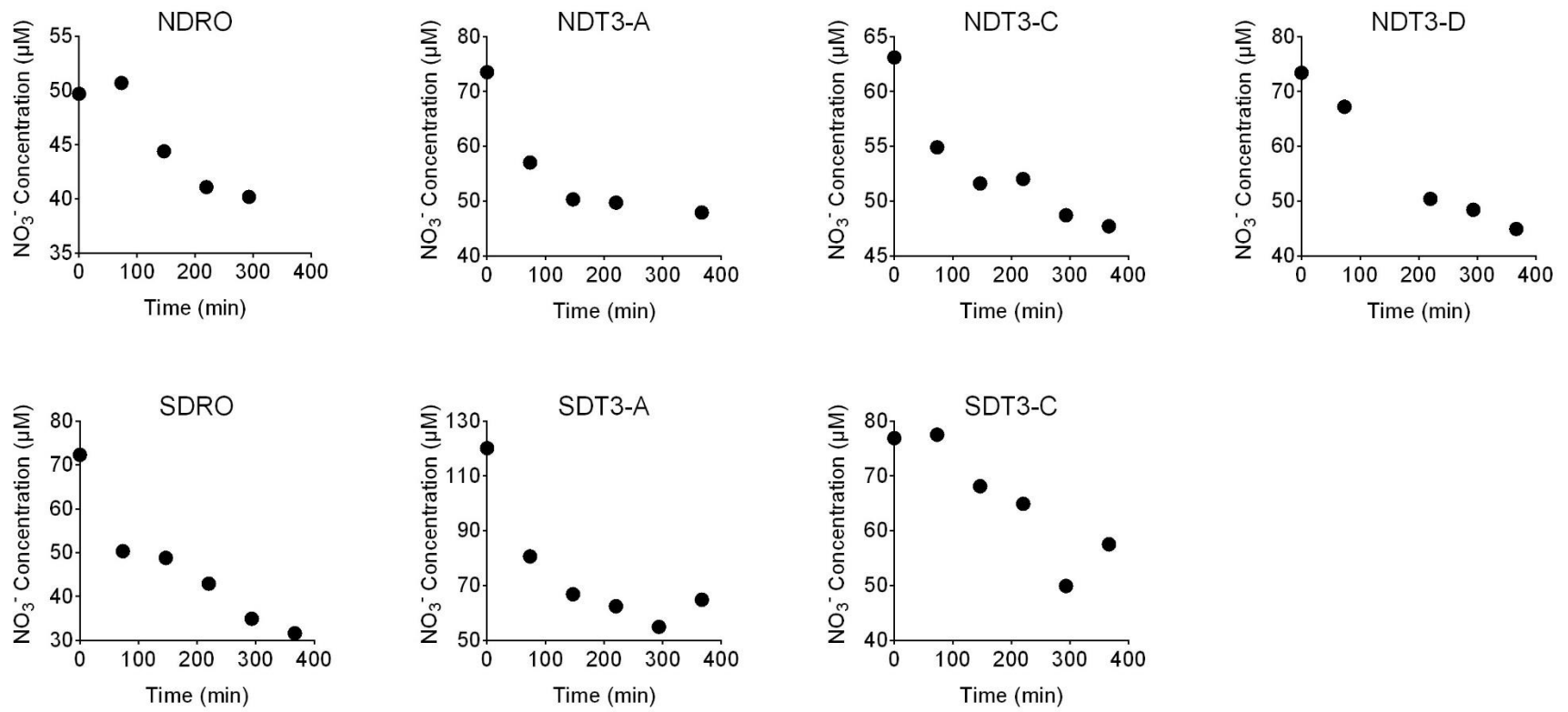
Figure S1. Nitrate (NO_3^-) concentrations in benthic flux chambers with $^{15}NO_3^-$ additions.
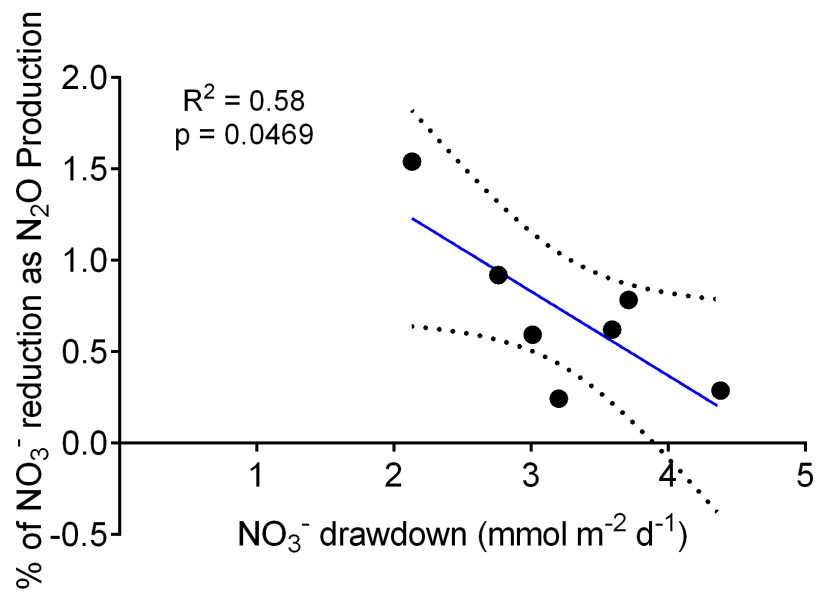
Figure S2. The correlation between NO_3^- drawdown rates measured from benthic flux chambers without $^{15}NO_3^-$ additions and the fraction of NO_3^- reduction as N_2O production. The solid line represents the best fit linear regression, and the dashed lines represent the 95% confidence interval band.
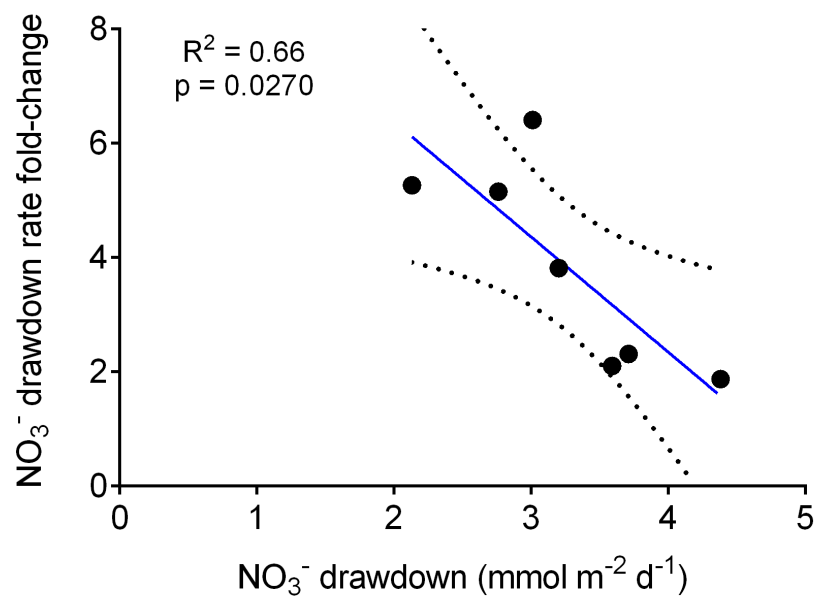
Figure S3. The correlation between NO_3^- drawdown rates measured from benthic flux chambers without $^{15}NO_3^-$ additions and the NO_3^- drawdown rate fold-change as a result of $^{15}NO_3^-$ additions (Table S2). The solid line represents the best fit linear regression, and the dashed lines represent the 95% confidence interval band.

Table S1. Detection limits of the rates of N_2 production from denitrification, N_2 production from anaerobic ammonia oxidation (anammox), NH_4^+ production from dissimilatory nitrate reduction to ammonia (DNRA), and N_2O production.

Station	NDT3-D	NDT3-C	NDT3-A	NDRO	SDRO	SDT3-A	SDT3-C
N_2 production - denitrification (mmol m^{-2} d^{-1})	0.053	0.174	0.092	0.156	0.200	0.042	0.051
N_2 production - anammox (mmol m^{-2} d^{-1})	0.027	0.083	0.032	0.238	0.202	0.033	0.041
NH_4^+ production from DNRA (mmol m^{-2} d^{-1})	0.006	0.022	0.026	0.018	0.071	0.010	0.029
N_2O production (µmol m^{-2} d^{-1})	2.46	1.46	1.11	1.25	5.60	3.94	2.94

Table S2. The fold change in bottom water NO_3^- concentration as a result of $^{15}NO_3^-$ addition; areal rates of NO_3^- drawdown with and without $^{15}NO_3^-$ addition and the calculated fold change.

Station	NDT3-D	NDT3-C	NDT3-A	NDRO	SDRO	SDT3-A	SDT3-C
NO_3^- fold change	1.99	1.62	1.90	2.75	6.17	3.43	2.30
NO_3^- drawdown rate without $^{15}NO_3^-$ addition (mmol m^{-2} d^{-1})	2.76	4.38	3.20	3.59	3.71	3.01	2.13
NO_3^- drawdown rate with $^{15}NO_3^-$ addition (mmol m^{-2} d^{-1})	14.22	8.19	12.21	7.53	8.58	19.26	11.22
NO_3^- drawdown rate fold change	5.15	1.87	3.81	2.10	2.31	6.40	5.26

Table S3. The contribution to $^{30}N_2$ production by anammox.

Station	NDT3-D	NDT3-C	NDT3-A	NDRO	SDRO	SDT3-A	SDT3-C
Contribution (%)	2.0%	1.9%	0.8%	1.5%	1.4%	0.9%	1.7%

Table S4. Bottom water nitrous oxide (N_2O) concentration and saturation at the beginning (T_0) of in-situ incubations. The saturation concentration of N_2O (12.16 nM) was calculated using the solubility equation from Weiss and Price (1980).

Station	NDT3-D	NDT3-C	NDT3-A	NDRO	SDRO	SDT3-A	SDT3-C
N_2O concentration (nM)	19.1	13.6	11.7	1.5	1.2	18.2	13.0
N_2O saturation	157%	112%	96%	12%	9%	150%	107%